View metadata, citation and similar papers at core.ac.uk

brought to you by CORE

provided by AIR Universita degli studi di Milano

First published April 1, 2009; doi:10.1152/jn.91190.2008.

Tonic Activation of $GABA_B$ Receptors Reduces Release Probability at Inhibitory Connections in the Cerebellar Glomerulus

Lisa Mapelli,[1,3] Paola Rossi,[1] Thierry Nieus,[2] and Egidio D'Angelo[1]

[1]*Department of Physiology and National Consortium for the Physics of Matter, University of Pavia, Pavia;* [2]*Italian Institute of Technology, Genoa, Italy; and* [3]*Department of Biomolecular Sciences and Biotechnology, University of Milan, Milan, Italy*

Submitted 7 November 2008; accepted in final form 26 March 2009

Mapelli L, Rossi P, Nieus T, D'Angelo E. Tonic activation of $GABA_B$ receptors reduces release probability at inhibitory connections in the cerebellar glomerulus. *J Neurophysiol* 101: 3089–3099, 2009. First published April 1, 2009; doi:10.1152/jn.91190.2008. In the cerebellum, granule cells are inhibited by Golgi cells through GABAergic synapses generating complex responses involving both phasic neurotransmitter release and the establishment of ambient γ-aminobutyric acid (GABA) levels. Although at this synapse the mechanisms of postsynaptic integration have been clarified to a considerable extent, the mechanisms of neurotransmitter release remained largely unknown. Here we have investigated the quantal properties of release during repetitive neurotransmission, revealing that tonic $GABA_B$ receptor activation by ambient GABA regulates release probability. Blocking $GABA_B$ receptors with CGP55845 enhanced the first inhibitory postsynaptic current (IPSC) and short-term depression in a train while reducing trial-to-trial variability and failures. The changes caused by CGP55845 were similar to those caused by increasing extracellular Ca^{2+} concentration, in agreement with a presynaptic $GABA_B$ receptor modulation of release probability. However, the slow tail following IPSC peak demonstrated a remarkable temporal summation and was not modified by CGP55845 or extracellular Ca^{2+} increase. This result shows that tonic activation of presynaptic $GABA_B$ receptors by ambient GABA selectively regulates the onset of inhibition bearing potential consequences for the dynamic regulation of signal transmission through the mossy fiber–granule cell pathway of the cerebellum.

INTRODUCTION

GABAergic synapses are endowed with a variety of γ-aminobutyric acid type A ($GABA_A$) receptor subtypes determining, in association with spillover and tonic GABA levels, the intensity and kinetics of inhibitory neurotransmission (Cherubini and Conti 2001; Farrant and Nusser 2005; Glykys and Mody 2007). $GABA_B$ receptors, in turn, can limit GABA release (Chen and Yung 2005; Deisz et al. 1997; Fearon et al. 2003; Jensen et al. 1999; Kaneda and Kita 2005; Morishita and Sastry 1995; Mouginot et al. 1998; Than and Szabo 2002) through a presynaptic mechanism. It has been proposed that, at central synapses, this mechanism could operate by reducing presynaptic calcium influx and synaptic vesicle recovery (Dittman and Regehr 1996; Sakaba and Neher 2003; Takahashi et al. 1998), thereby regulating the dynamics of repetitive neurotransmission (Hefft et al. 2002). However, the impact of this change is likely to depend on the specific property of synapses, including their presynaptic dynamics, the $GABA_A$ receptor subtypes, the amount of neurotransmitter spillover, and the tonic GABA level.

Address for reprint requests and other correspondence: E. D'Angelo, Department of Physiological and Pharmacological Sciences and National Consortium for the Physics of Matter, University of Pavia, Via Forlanini 6, I-27100 Pavia, Italy (E-mail: dangelo@unipv.it).

Along the mossy fiber pathway of cerebellum, GABAergic synapses are formed between Golgi cells and granule cells inside the glomeruli. In response to stimulation, inhibition arises rapidly with millisecond precision before slowly degrading over about 100 ms (in vivo: Eccles et al. 1967; in vitro: Maffei et al. 2002). The Golgi cells are spontaneously active at low frequency (Forti et al. 2006; Solinas et al. 2008a,b) and respond to punctuate stimulation with brief spike bursts (Vos et al. 1999). The granule cells are activated by the mossy fibers (D'Angelo et al. 1993, 1995, 1999, 2001; Nieus et al. 2006; Rossi et al. 2006; Sola et al. 2004) and their activity is limited by the feedforward and feedback inhibitory loops formed by Golgi cells. In granule cells, α_1 and α_6 subunit-containing $GABA_A$ receptors (Brickley et al. 1999; Farrant and Nusser 2005) generate fast and slow inhibitory postsynaptic current (IPSC) components in response to direct release onto postsynaptic densities and spillover from neighboring contacts (Hamann et al. 2002; Rossi and Hamann 1998; Rossi et al. 2003). In addition, ambient GABA at submicromolar concentration activates high-affinity α_6 $GABA_A$ receptors generating tonic inhibition. This latter has been shown to regulate the input–output relationship of the granule cell (Brickley et al. 1996) and has been proposed to control the mossy fiber–granule cell gain (Mitchell and Silver 2003). However, it is unknown whether $GABA_B$ receptors, which are present in Golgi cells (Kulik et al. 2002) and have affinities in the same GABA concentration range (Galvez et al. 2000), could also be activated presynaptically and regulate neurotransmitter release. This potential regulation, given the multiple types and different activation modes of postsynaptic receptors, is expected to exert complex effects on repetitive Golgi cell–granule cell neurotransmission.

Herein we report a novel mechanism for tonic GABA levels in the cerebellar glomerulus. In juvenile rats, $GABA_B$ receptors exerted a tonic depression on release probability at the Golgi cell–granule cell synapse. The main consequence was that of reducing the first response without substantially altering the total inhibitory charge in a train. It is therefore proposed that ambient GABA, by acting through presynaptic $GABA_B$ receptors, selectively regulates the sharpness of the onset of inhibition in granule cells. The potential consequences for signal transmission along the mossy fiber pathway are discussed.

METHODS

Slice preparation and solutions

Patch-clamp recordings in acute cerebellar slices were performed as previously reported (Armano et al. 2000; D'Angelo et al. 1993, 1995,

0022-3077/09 $8.00 Copyright © 2009 The American Physiological Society

Downloaded from www.physiology.org/journal/jn by ${individualUser.givenNames} ${individualUser.surname} (094.161.143.194) on April 5, 2018.
Copyright © 2009 American Physiological Society. All rights reserved.

1999). Briefly, 17- to 23-day-old Wistar rats were anesthetized with halothane (Aldrich, Milwaukee, WI) and killed by decapitation. Acute 220-μm-thick slices were cut in the sagittal plane from the cerebellar vermis in cold Krebs solution and maintained at 30°C before being transferred to a 1.5-ml recording chamber mounted on the stage of an upright microscope (Olympus BX51WI, Tokyo, Japan). The preparations were perfused with Krebs solution (2 ml/min) and maintained at 30°C with a Peltier feedback device (TC-324B, Warner Instruments, Hamden, CT).

Krebs solution for slice cutting and recovery contained (in mM): 120 NaCl, 2 KCl, 1.2 $MgSO_4$, 26 $NaHCO_3$, 1.2 KH_2PO_4, 2 $CaCl_2$, and 11 glucose, and was equilibrated with 95% O_2-5% CO_2 (pH 7.4). During recordings, the glutamate receptor blockers 6-cyano-7-nitroquinoxaline-2,3-dione (CNQX), 2-amino-5-phosphonovaleric acid (APV), 7-chlorokynurenic acid (7-Cl-Kyn), and (*RS*)-1-amino-indan-1,5-dicarboxylic acid (AIDA) were applied through a local perfusion pipette. In some experiments, slices were preincubated with a low-Ca^{2+} solution and Ca^{2+} concentration was changed by both local and bulk bath perfusion. Krebs solutions with different Ca^{2+} concentrations (from 0.5 to 4 mM) were prepared, maintaining constant the total concentration of divalent cations by corresponding changes in Mg^{2+} (with 6 mM Ca^{2+} no Mg^{2+} was added). The patch-clamp pipette solution contained (in mM): 81 Cs_2SO_4, 4 NaCl, 2 $MgSO_4$, 0.02 $CaCl_2$, 0.1 BAPTA, 15 glucose, 3 ATP-Mg, 0.1 GTP, and 15 HEPES. This solution maintained resting free [Ca^{2+}] at 100 nM and pH was adjusted to 7.2 with CsOH. Patch-clamp pipettes filled with this solution had a resistance of 5–8 MΩ before seal formation. All drugs were obtained from Sigma, except BAPTA tetrapotassium salt (Molecular Probes, Eugene, OR); CNQX, APV, 7-Cl-Kyn, AIDA, and $GABA_A$ receptor blocker bicuculline (Tocris-Cookson, Avonmouth, UK), and tetrodotoxin (TTX; Latoxan, Valence, France).

Data recording and analysis

In this study we have recorded miniature synaptic currents (mIPSCs), spontaneous synaptic currents (sIPSCs), and evoked synaptic currents (eIPSCs) from granule cells. Granule cells were voltage-clamped at −10 mV with an Axopatch 200-B amplifier and currents sampled with a Digitada 1440-A interface (low-pass filter = 10 kHz; sampling rate = 100 kHz). Golgi cell axon bundles were stimulated with a patch-pipette via an isolation unit at a frequency of 0.1–0.33 Hz. The acquisition program automatically switched between eIPSC and background activity recordings (for 3 to 10 s), from which sIPSCs and mIPSCs were detected. IPSCs were digitally filtered at 1.5 kHz and analyzed off-line with pCLAMP (Axon Instruments software). Peak amplitude, time to peak (ttp), rise time from 10 to 90% of peak amplitude (RT_{10-90}), and duration at half-width (HW) were computed. The paired-pulse ratio (PPR) between the first and second IPSCs in a sequence was PPR = $IPSC_2/IPSC_1$. To minimize the impact of stimulus artifact in eIPSC trains, exponential fitting to response decay was extrapolated to find the baseline from which the amplitude in the subsequent response was measured.

sIPSC and mIPSC analyses were performed automatically with Clampfit software, setting a proper threshold for event detection; a further visual inspection of detected signals allowed us to reject noisy artifacts. A 10-min period was adopted to evaluate mean eIPSC amplitude and coefficient of variation (CV); longer periods did not usually improve the estimate. The error introduced in eIPSC CV by the indirect response, which causes nonzero failures (see Fig. 1*D*), was eliminated by setting all indirect responses to zero (these were identified because the lack of the transient component caused a distinct population of small and slow IPSCs in amplitude/RT_{10-90} plots; data not shown).

Since the stability of synaptic transmission can be influenced by slow modifications of neurotransmitter release and series resistance, response stability was assessed from average eIPSC amplitudes over 3-min periods (Larkman et al. 1992). The average eIPSC amplitude changed by <10% over the time windows used for statistical analysis. The series resistance was monitored by measuring passive current transients induced by 10-mV hyperpolarizing voltage steps from a holding potential of −60 mV. The cerebellar granule cell has a compact structure and behaves like a single electrotonic compartment (Cathala et al. 2003; D'Angelo et al. 1993, 1995; Silver et al. 1996). Accordingly, the transients were reliably fitted with a monoexponential function, yielding membrane capacitance $C_m = 4.3 \pm 0.1$ pF ($n = 29$), membrane resistance $R_m = 2.7 \pm 0.3$ GΩ ($n = 29$), and series resistance $R_s = 17.3 \pm 1.1$ MΩ ($n = 29$). The −3-dB cell + electrode cutoff frequency was $f_{VC} = (2\pi R_s C_m)^{-1} = 2.4 \pm 0.1$ kHz ($n = 29$). Accepted deviations of these parameters in current transients recorded over the time windows used for statistical analysis were <10%.

Data are reported as means ± mean squared error (MSE) and, unless otherwise indicated, statistical comparisons are done using Student's *t*-test.

Identification of minimal IPSCs

At several central synapses, identification of minimal stimulation requires adopting indirect statistical methods like establishing a certain percentage of successful responses to stimulation, often preventing establishing an accurate estimate of release failure rate and release probability. The glomerular synapses in the cerebellum, by being composed of a very few (just two to four; Hámori and Somogyi 1983; Harvey and Napper 1991) contacts per granule cell, proves convenient in overcoming these difficulties. At the excitatory connection between mossy fibers and granule cells, the intensity of stimulation can be finely tuned by "counting" the discrete levels of the response amplitude and selecting the minimal one (Saviane and Silver 2006a,b; Sola et al. 2004). At the inhibitory connections investigated here, minimal eIPSCs were similarly obtained by finely tuning the stimulation intensity. In addition, minimal eIPSC amplitude was systematically compared with that of sIPSCs, which are due to the activation of single Golgi cell contacts. Therefore a post hoc criterion could be applied, in that minimal eIPSCs had to be statistically indistinguishable from sIPSCs; otherwise, the recording was not further considered for quantal analysis. An additional advantage was that of identifying stimulation failures from the absence of the slow spillover-dependent "*indirect component*," thereby improving the confidence in release probability estimates and allowing application of the "failure method" (see *Eq. 3* in the following text). Finally, the limited number of synaptic contacts and the favorable electrotonic properties of recordings allow establishing a reliable estimate of quantum properties from mIPSCs.

Binomial release statistics

The quantal parameters of release were obtained by applying to minimal eIPSCs three statistical methods corresponding to *Eq. 1*, *Eq. 2*, and *Eq. 3* to improve the reliability of parameter estimation. These methods derive from binomial statistics and are only schematically described here, since they do not significantly differ from previous applications (for a comprehensive treatment see Clements 2003; Clements and Silver 2000; McLachlan 1978; Sola et al. 2004).

The quantal theory states that the mean number of quanta released at each impulse (m, mean quantum content) depends on the number of releasing sites (n) and on the probability (p) that each quantum (q, quantum size) is released, so that eIPSC variance ($S^2 = SD^2$) and mean amplitude ($M = mq$) are related through a parabolic function and eIPSC variability depends on the number of released quanta. The contribution of intrinsic quantum variability can be accounted for by identifying intrasite (type I) and intersite (type II) sources. Intrasite variability (cv_I) reflects fluctuation in the number of open channels at single sites ($cv_{I\text{-}ss}$) and asynchrony in quantal delay at the eIPSC peak ($cv_{I\text{-}qd}$). Intersite variability (cv_{II}) reflects differences among postsynaptic densities. Thus the total quantal variance at the eIPSC peak can be expressed as $cv^2_{tot} = cv^2_I + cv^2_{II} = (cv^2_{I\text{-}ss} + cv^2_{I\text{-}qd}) + cv^2_{II}$. The variability of mIPSCs (cv_q) includes intrasite and intersite quantal variability, $cv^2_q = cv^2_{I\text{-}ss} + cv^2_{II}$. Since $cv^2_{I\text{-}ss}$ can be assumed to be similar to cv^2_{II} (for details see

Downloaded from www.physiology.org/journal/jn by ${individualUser.givenNames} ${individualUser.surname} (094.161.143.194) on April 5, 2018.
Copyright © 2009 American Physiological Society. All rights reserved.

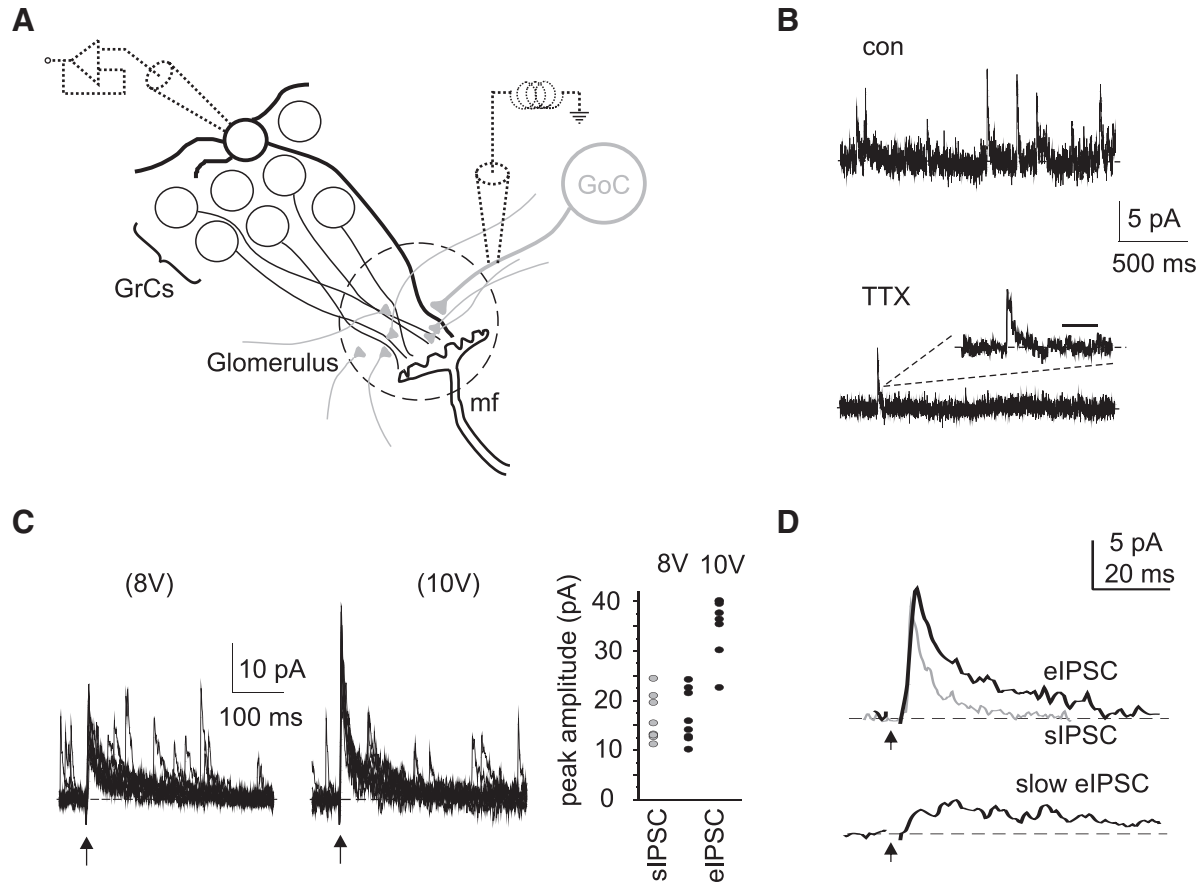

FIG. 1. Golgi cell–granule cell inhibitory currents. *A*: schematic drawing of glomerular synapses. In the glomerulus (dashed circle), granule cell (GrC) dendrites make synaptic contact with a mossy fiber (mf) terminal as well as with Golgi cell (GoC) axon fibers (gray). A granule cell dendrite can receive GABAergic inhibition through direct release of γ-aminobutyric acid (GABA) from the corresponding GoC synaptic contact or through diffusion of GABA from synapses formed by axonal branches on neighboring dendrites in the glomerulus. Electrical stimuli were applied in the surrounding neuropile activating axons of the Golgi cells, while recording from a granule cell. Excitatory transmission was blocked by perfusing glutamate receptor antagonists. *B*: spontaneous activity recorded from a granule cell at −10 mV. The spontaneous inhibitory postsynaptic currents (sIPSCs) disappeared during 1 μM tetrodotoxin (TTX) perfusion, leaving rare miniature IPSCs (mIPSCs, magnified in the *inset*). Note also that background noise decreased during TTX perfusion, presumably reflecting a reduction of tonic GABA receptor activation by ambient GABA. *C*: evoked IPSCs (eIPSCs) following electrical stimulation (arrows). The eIPSCs were elicited first by using minimal stimulation (set as explained in METHODS) and then after raising the stimulation intensity (from 8 to 10 V) in the same cell. The scatterplot shows the amplitude of sIPSCs and eIPSCs for the same tracings shown at the *left*. *D*: minimal eIPSC (*black trace*) and sIPSC (*gray trace*) are shown superimposed. Note that sIPSC has faster decay kinetics than that of minimal eIPSC. The slow eIPSCs are shown at the *bottom*. These traces are averages of 6 recordings from the same cell.

Clements 2003), we equally divided the two terms as $cv^2_{I\text{-}ss} \approx cv^2_{II} = 1/2cv^2_q$. The limits of this assumption were assessed by calculating the error introduced by setting $cv^2_{I\text{-}ss}$ at its extreme values (either $cv^2_{I\text{-}ss} = 0$ or $cv^2_{I\text{-}ss} = cv^2_q$). The term $cv_{I\text{-}qd}$ was obtained by measuring the difference in variance associated with stimulus-aligned eIPSCs compared with onset-aligned quantal eIPSCs in low Ca^{2+} solutions (as proposed by Clements and Silver 2000). Thus $cv^2_I \approx 1/2cv^2_q + cv^2_{I\text{-}qd}$ (parameter value estimates are reported in Figs. 1–3).

The relationship between eIPSC S^2 and M, constructed by using different Ca^{2+} concentrations in the extracellular solution, was analyzed using a binomial model under the assumption of homogeneous release probability (this was supported by the substantial symmetry of the data distribution; see Clements and Silver 2000 and Fig. 4*A*)

$$S^2 = q_p M(1 + cv_I^2) - \frac{M^2}{n} \quad (1)$$

The model can also be applied without a knowledge of the whole variance/mean distribution (McLachlan 1978), since the parameters p and n can be calculated from the mean amplitude and coefficient of variation of eIPSCs ($M = mq_p$ and $CV = S/M$, where S is eIPSC SD). In this model $m = np$, $SD^2 = np(1 - p)$, and the probability p is

$$p^2 = 1 - \frac{M(CV^2)}{q_p(1 + cv_I^2)} \quad (2)$$

An estimate of p could also be obtained from the failure rate (N_0/N; N_0 represents the failures out of N responses), which does not explicitly depend on previous determinations of quantum properties except that the number of releasing sites needs to be calculated beforehand with *Eq. 1* or *Eq. 2*

$$p = 1 - (N_0/N)^{1/n} \quad (3)$$

Although the three methods have different dependencies on experimental measurements and different intrinsic estimation errors (McLachian 1978), they yielded very similar parameter values (see Fig. 4*B*), thus supporting the reliability of p estimates.

RESULTS

Herein we have investigated Golgi cell–granule cell neurotransmission and its modulation by GABA$_B$ receptors in acute cerebellar slices (the synaptic organization of inhibi-

Downloaded from www.physiology.org/journal/jn by ${individualUser.givenNames} ${individualUser.surname} (094.161.143.194) on April 5, 2018.
Copyright © 2009 American Physiological Society. All rights reserved.

tion in the cerebellar glomerulus is summarized in Fig. 1*A*). Whole cell recordings were performed in the presence of glutamate receptor antagonists to block excitatory synaptic transmission.

The granule cells usually showed spontaneous activity (Fig. 1*B*) characterized by inhibitory synaptic currents occurring at an average frequency of 4.22 ± 0.81 Hz (n = 25). Most (>98%) of these events disappeared during application of 1 μM TTX, which suppresses spontaneous Golgi cell activity (Forti et al. 2006). Thus these events were most likely to represent unitary spontaneous current (*sIPSC*) generated at individual Golgi cell–granule cell connections. The rare TTX-*in*sensitive spontaneous events (0.066 ± 0.008 Hz, n = 9, 1.6% of all the spontaneous events) were identified as miniature synaptic currents (*mIPSCs*). Electrical stimulation of the neuropile (Fig. 1*C*) evoked inhibitory synaptic currents (*eIPSCs*). Any synaptically related activities were abolished by 10 μM bicuculline and were therefore fully mediated by $GABA_A$ receptors (n = 5; data not shown). These results confirm the absence of slow $GABA_B$ receptor-mediated responses in granule cell inhibitory currents (Rossi et al. 2006; for different neurons: Dutar and Nicoll 1998; Misgeld et al. 1995; Nicoll 2004).

In the glomerulus, numerous synaptic terminals and granule cell dendrites are enwrapped in a glial sheet that limits neurotransmitter diffusion (Fig. 1*A*). This arrangement was previously shown to cause evident effects on $GABA_A$ receptor-mediated neurotransmission: whereas sIPSCs and a fast transient component of eIPSCs proved dependent on *direct* release onto the postsynaptic site, the slow eIPSC tail turned out to be generated by *indirect* activation through spillover (Brickley et al. 1996; Rossi and Hamann 1998). Consistently, in our recordings (Fig. 1*D*) sIPSCs lacked the slow sustained tail that characterizes eIPSCs (HW = 4.44 ± 0.52 vs. 13.61 ± 2.43 ms, n = 6) and the indirect component emerged in isolation when the direct component failed. The transient component arose rapidly, with a ttp value varying between 0.5 and 2 ms (Tia et al. 1996). The duration of the rising phase was not limited by the recording system (which ensured 100-μs resolution; see METHODS and Sola et al. 2004) and probably reflected the time needed for receptor opening and asynchronies due to multiquantal release (see following text and Fig. 2).

Evidence for multiquantal evoked release

The glomerular synapse offers a convenient model for assessing the quantal properties of neurotransmission, since it allows easy identification of the eIPSCs generated at unitary synaptic connections, to distinguish transmission from stimulation failures and to directly estimate single quantum properties (see METHODS). First, the amplitude of eIPSCs elicited by minimal stimulation was statistically indistinguishable from that of sIPSCs (in the same cells: 13.83 ± 0.95 vs. 15.94 ± 1.45 pA; ratio = 1.12 ± 0.07; n = 16; P = 0.2, paired t-test), consistent with an origin of both sIPSCs and minimal eIPSCs from *unitary synaptic connections* (Fig. 1*C*). This condition was assessed systematically: by increasing stimulus intensity, eIPSCs outranged sIPSCs (40.3 ± 4.9 pA, n = 13), indicating recruitment of additional connections (Hámori and Somogyi 1983; Harvey and Napper 1991). In continuation of this work, we will exclusively consider eIPSCs elicited by minimal stimulation and therefore presumably arising from single connections. Second, the occurrence of the indirect component in isolation allowed us to identify *release failures* at the site under investigation and to exclude potential stimulation failures (Fig. 1*D*; cf. DiGregorio et al. 2002; Sola et al. 2004). Third, the mIPSCs did not show indents in their rising phase (Fig. 2*A*), suggesting that they originated from release of single *neurotransmitter quanta* (e.g., see Cathala et al. 2003), whereas indents could often be observed in the sIPSCs and eIPSCs. The mIPSCs were thus used to estimate the quantum size (q = 8.47 ± 0.94 pA, n = 9) and coefficient of variation (cv_q = 0.29 ± 0.12, n = 9).

The quantal nature of GABAergic neurotransmission at the glomerular synapse was further investigated by perfusing solutions containing variable Ca^{2+}/Mg^{2+} proportions (Dittman and Regehr 1996; Dodge Jr and Rahamimoff 1967; Katz and Miledi 1967). In normal extracellular calcium (2 mM Ca^{2+}), the eIPSCs showed pronounced trial-to-trial amplitude fluctuations with CV (0.61 ± 0.09, n = 6), which was significantly larger than cv_q (P < 0.01, unpaired t-test, n = 6 and 9), indicating that eIPSCs were generated by release of multiple quanta (Fig. 2*B*). In low extracellular Ca^{2+} (0.5 mM Ca^{2+}), when release tends to occur at single releasing sites or to fail, eIPSC amplitude (10.58 ± 1.26, n = 6, failures excluded) was statistically indistinguishable from that of mIPSC (P = 0.19, unpaired t-test, n = 6 and 9) (Fig. 2*C*). The increase of

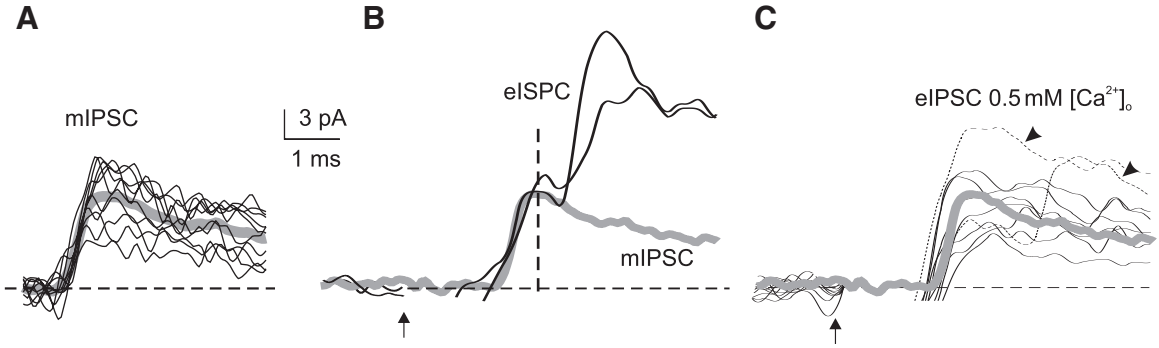

FIG. 2. Quantal components of the inhibitory response. *A*: the mIPSCs (10 traces) show amplitude fluctuations. The average mIPSC is shown in gray and replotted in the next 2 panels. *B*: 2 single minimal eIPSCs show a marked indent in their rising phase. The indent overlaps with the average mIPSC. *C*: the amplitude of most eIPSCs recorded in 0.5 mM extracellular calcium ion concentration ($[Ca^{2+}]_o$) does not differ significantly from that of mIPSCs, although some of them (dashed traces with arrowheads) could be biquantal. The failure rate in this cell was 50%. The mIPSCs in *A* were obtained from a cell different from that in *B* and *C*. The arrows indicate the time of synaptic stimulation.

Downloaded from www.physiology.org/journal/jn by ${individualUser.givenNames} ${individualUser.surname} (094.161.143.194) on April 5, 2018.
Copyright © 2009 American Physiological Society. All rights reserved.

extracellular Ca^{2+} from 0.5 to 6 mM progressively increased the eIPSC mean amplitude (Fig. 3*A*). Moreover, the eIPSC amplitude distribution became broader and its mode moved to the right. Finally, the failures and CV were reduced (Fig. 3*B*). These observations indicate a mechanism in which GABA is released in multiple quanta during evoked neurotransmission at unitary synaptic connections and release probability is controlled by calcium (Edwards et al. 1990; Takahashi et al. 1998).

Statistical properties of Golgi cell–granule cell neurotransmission

The results shown in Figs. 1–3 suggest that eIPSC variability is caused both by intrinsic quantal variability and by the different number of quanta released from trial to trial. Information on *quantal variability* was provided by mIPSCs and mono-quantal eIPSCs in low Ca^{2+}. The mIPSCs are generated at all synaptic sites impinging on the granule cell, so that their amplitude fluctuates because of variability originating within single sites ($cv_{I\text{-}ss}$) and across different sites (cv_{II}). Since no measures of $cv_{I\text{-}ss}$ were available, we considered that $cv^2_{I\text{-}ss}$ and cv^2_{II} equally contributed to the quantal variability cv_q, so that $cv^2_{I\text{-}ss} \approx cv^2_{II} = 1/2cv^2_q = 0.043$ (Clements 2003; this assumption is tested in the following text). An additional factor that can affect the contribution of quanta to eIPSCs is the time scatter in quantal release observed in Fig. 2*A*. In mono-quantal eIPSCs, which are presumably generated at single sites of just one of the synapses impinging on the granule cell, the time scatter of evoked quantal release can be measured by comparing peak-aligned to stimulus-aligned eIPSCs (see METHODS). This scatter causes a reduction of the eIPSC peak by 17.5 ± 2.8% ($n = 6$) and allows us to estimate the variability of quantum delay (qd), $cv^2_{I\text{-}qd} = 0.03 \pm 0.04$ ($n = 6$). This term adds to the intrasite variance, which then becomes $cv^2_I = cv^2_{I\text{-}ss} + cv^2_{I\text{-}qd} \approx 1/2cv^2_q + cv^2_{I\text{-}qd} = 0.073$.

The *eIPSC variability* was investigated by constructing a variance/mean plot, in which eIPSC mean amplitude was changed by varying extracellular Ca^{2+} concentration (multiple-probability fluctuation analysis [MPFA]: Clements and Silver 2000; Silver 2003; Silver et al. 1996; Sola et al. 2004). The data were pooled from 20 recordings (Fig. 4*A*) belonging to experiments, in which several different Ca^{2+} concentrations were tested (1, 2, 4, and 6 mM). The plot showed a parabolic shape with downward concavity and was fitted with *Eq. 1*, yielding values for the quantum size at eIPSC peak, $q_p = 10.71 \pm 1.29$ pA and the number of releasing sites, $n = 4.66 \pm 0.76$. The calculated average p value in 2 mM Ca^{2+} was 0.31 ± 0.12. Results of MPFA (*Eq. 1*) were compared with those obtained using the CV method (*Eq. 2*) and the failure method (*Eq. 3*). At 2 mM Ca^{2+} ($n = 5$), *Eq. 2* yielded $n = 5.76 \pm 0.53$ and $p = 0.33 \pm 0.03$ (q was taken from minis; see Figs. 1 and 2). With the n value calculated from *Eq. 2* and the failure rate, *Eq. 3* yielded $p = 0.31 \pm 0.14$. These calculations were extended over the whole Ca^{2+} concentration range that was investigated and, consistently,

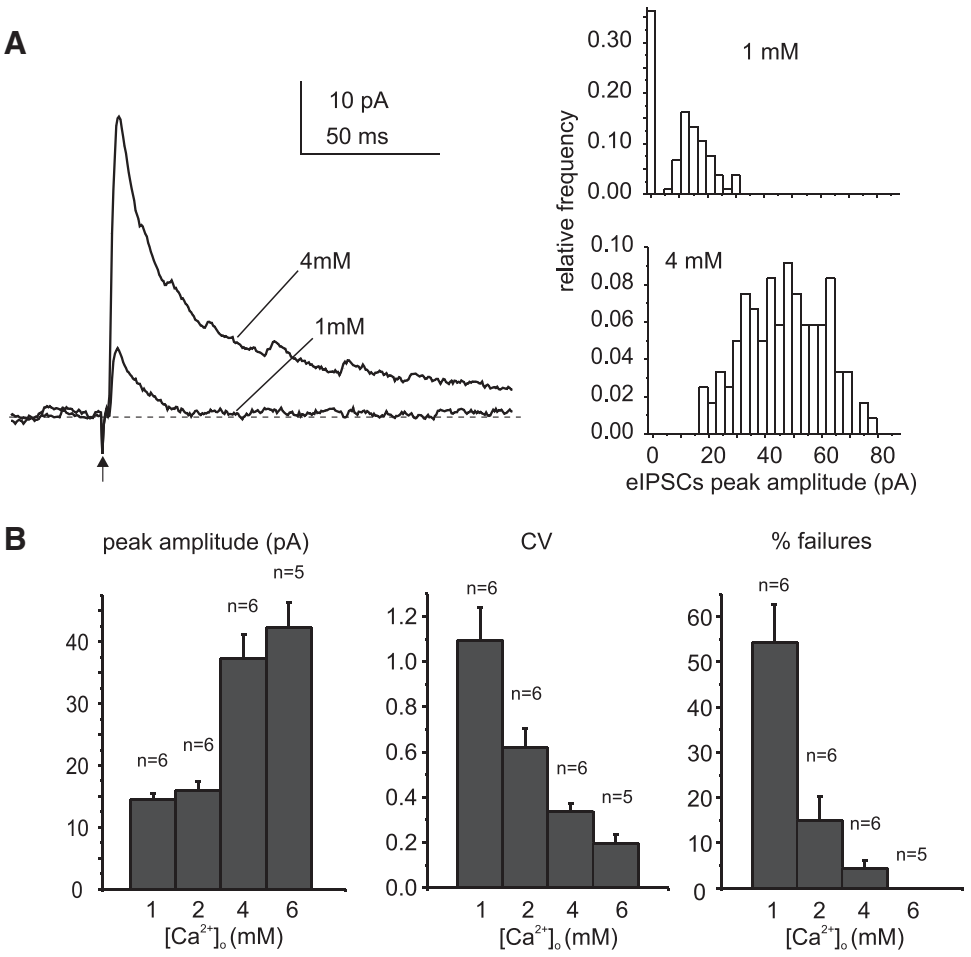

FIG. 3. Dependence of eIPSCs on $[Ca^{2+}]_o$. *A*: average minimal eIPSCs (averages of 10 traces) are increased when passing from 1 to 4 mM $[Ca^{2+}]_o$ (the arrow indicates synaptic stimulation). The histograms show the amplitude distributions for the same recordings. Note the decrease in failures and the shift of the distribution to the *right* when $[Ca^{2+}]_o$ is increased. Each histogram is made of 125 responses (3-pA bin size) and no clear quantal peaks can be observed. *B*: histograms of minimal eIPSC peak amplitude (*left*), coefficient of variation (CV, failures included, *middle*), and failure rate (*right*), at the different $[Ca^{2+}]_o$ tested. At 0.5 mM Ca^{2+} eIPSCs failures were so numerous to preclude CV calculation. Values are reported as mean ± mean standard error (MSE).

Downloaded from www.physiology.org/journal/jn by ${individualUser.givenNames} ${individualUser.surname} (094.161.143.194) on April 5, 2018.
Copyright © 2009 American Physiological Society. All rights reserved.

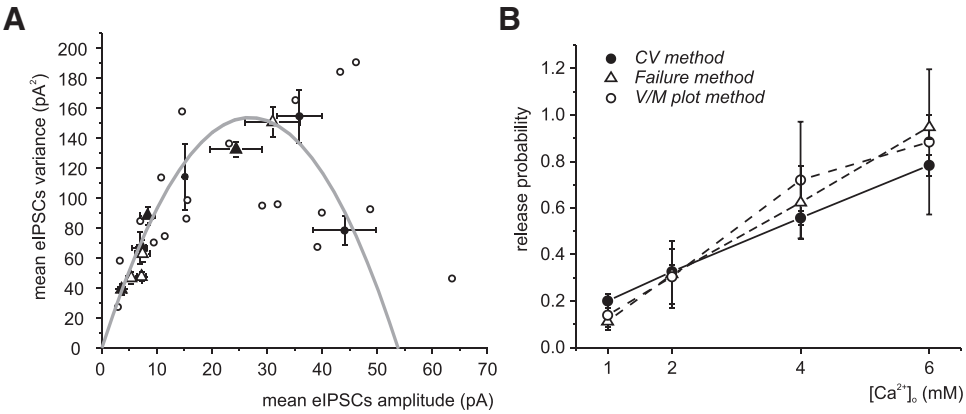

FIG. 4. Variance–mean plot and p estimates. *A*: a variance–mean plot was constructed using minimal eIPSCs taken from 20 granule cells recorded with 1, 2, 4, and 6 mM $[Ca^{2+}]_o$ (open circles are single-cell values, filled circles are average values ± MSE, $n = 5$, corresponding to different $[Ca^{2+}]_o$). The data were fitted with a parabolic function (*Eq. 1*, gray line; $q_p = 10.71 \pm 1.29$ pA, $n = 4.66 \pm 0.76$, $cv_I^2 = 0.073$; $R^2 = 0.87$, $P < 0.05$, paired t-test). The points corresponding to 4 subsequent responses in a 100-Hz train (control, filled triangles; CGP55845, open triangles; mean ± MSE, $n = 5$, same cells as in Figs. 6 and 7) fall on the same parabolic trajectory. *B*: release probability estimated with 3 different methods (*Eq. 1*, open circles; *Eq. 2*, filled circles; *Eq. 3*, open triangles) at different values of $[Ca^{2+}]_o$. The 3 estimates were similar for all $[Ca^{2+}]_o$ values.

all the methods yielded similar p values, thus supporting the reliability of estimates (Fig. 4*B*).

The impact of the assumption that $cv_{I\text{-}ss}^2 \approx cv_{II}^2 = 1/2cv_q^2$ (Clements 2003) was evaluated by setting either $cv_{I\text{-}ss} = 0$ or $cv_{I\text{-}ss}^2 = cv_q$. With *Eq. 1*, the error introduced by setting $cv_{I\text{-}ss} = 0$ was +1% for q and <1% for both p and n; the error introduced by setting $cv_{I\text{-}ss} = cv_q$ was −7% for q and <1% for both p and n. With *Eq. 2*, the error introduced by setting $cv_{I\text{-}ss} = 0$ was +15% for p and −18% for n; the error introduced by setting $cv_{I\text{-}ss} = cv_q$ was −2% for p and 2% for n. With *Eq. 3*, the dependence on cv is indirect and passes through the n value estimated with *Eq. 2*. The error propagated from *Eq. 2* to *Eq. 3* was 17%, by setting $cv_{I\text{-}ss} = 0$ and −1.6% by setting $cv_{I\text{-}ss} = cv_q$. Therefore the assumption about single quantum variability introduced relatively little error on p, n, and q estimates.

Short-term plasticity during repetitive stimulation

Golgi cells usually respond to punctuate stimulation with short high-frequency spike bursts (Rancz et al. 2007; Solinas et al. 2007a,b; Vos et al. 1999). To imitate native Golgi cell patterns, we tested the effect of five-impulse 100-Hz stimulus trains (Fig. 5).

In normal calcium (2 mM), the transient eIPSC component showed a clear depression, whereas the persistent component showed a pronounced buildup. In the transient component, PPR = 0.50 ± 0.09 ($n = 8$) was measured on the first two eIPSCs. In low calcium (0.5 mM), the initial depression turned into facilitation, yielding a PPR = 1.50 ± 0.35 ($n = 5$) on the first two eIPSCs. At both calcium concentrations, the eIPSC tended to similar and constant amplitude in the third and fourth responses. Thus as at other synapses (e.g., the neighboring mossy fiber–granule cell synapse; see Sola et al. 2004), facilitation and depression coexisted but, at normal calcium, depression prevailed.

The five neurons covered in this section are a subpopulation of the larger sample reported in Fig. 4. Consistent with the behavior reported in Fig. 4, release probability computed using *Eq. 2* on the first eIPSC in the trains changed from $p = 0.42 \pm 0.06$ in 2 mM calcium to $p = 0.23 \pm 0.05$ in 0.5 mM calcium ($n = 5$). Moreover, the variance/mean points obtained for subsequent eIPSCs during the trains also fell along the parabolic trajectory obtained by changing Ca^{2+} concentration (Fig. 4*A*), thus indicating that a progressive reduction in the number of released quanta was the main determinant of eIPSC short-term depression.

Modulation of inhibitory neurotransmission by $GABA_B$ receptors

At various GABAergic synapses, neurotransmitter release has been reported to undergo negative modulation through $GABA_B$ autoreceptors (Dittman and Regehr 1996; Sakaba and Neher 2003; Takahashi et al. 1998). It is therefore possible that $GABA_B$ receptors, which are expressed in Golgi cells (Kulik et al. 2002), also control GABA release from Golgi cell terminals. To investigate this hypothesis, we perfused the

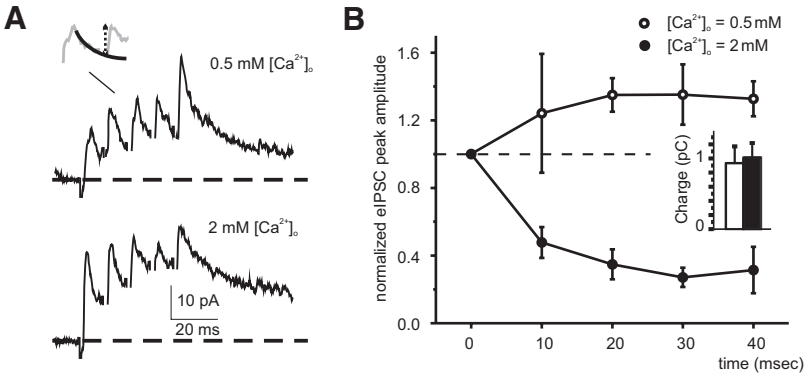

FIG. 5. Short-term plasticity during repetitive synaptic stimulation. *A*: the traces show the eIPSCs elicited by short 100-Hz trains (averaging of 20 responses) taken at 0.5 mM $[Ca^{2+}]_o$ and 2 mM $[Ca^{2+}]_o$ from the same cell. Whereas short-term facilitation appears at 0.5 mM $[Ca^{2+}]_o$, the response shows short-term depression of peak amplitude at 2 mM $[Ca^{2+}]_o$. The *inset* shows exponential fitting to the decay of an IPSC in the train, which was needed to determine the baseline from which the amplitude of the subsequent IPSC could be measured. *B*: plot of normalized eIPSC peak amplitude (mean ± MSE) in the train for 8 experiments, like those shown in *A* (0.5 mM $[Ca^{2+}]_o$, $n = 5$; 2 mM $[Ca^{2+}]_o$, $n = 8$). The histogram represents the charge transfer during the trains. Despite different short-term dynamics, no relevant difference in charge transfer was observed between 0.5 mM $[Ca^{2+}]_o$ (white bar) and 2 mM $[Ca^{2+}]_o$ (black bar) ($P = 0.58$, unpaired t-test).

Downloaded from www.physiology.org/journal/jn by ${individualUser.givenNames} ${individualUser.surname} (094.161.143.194) on April 5, 2018.
Copyright © 2009 American Physiological Society. All rights reserved.

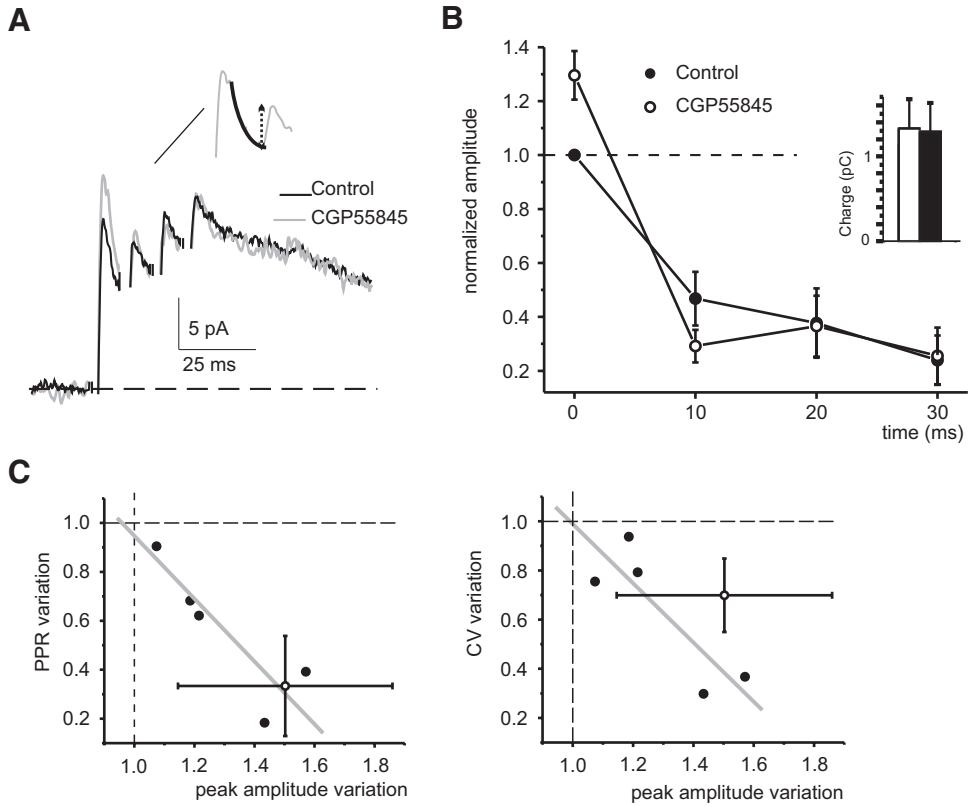

FIG. 6. Modulation of inhibitory transmission by GABA$_B$ receptors. *A*: the traces show the minimal eIPSCs elicited by short 100-Hz trains (averaging of 30 responses) taken in control and after perfusion of CGP55845 (1 μM). The control (black) and CGP55845 (gray) traces are superimposed to show the relative changes in the eIPSC amplitude. Note that the 1st eIPSC increased but then the response tended to a common steady state. The *inset* shows exponential fitting to the decay of an IPSC in the train, which was needed to determine the baseline from which the amplitude of the subsequent IPSC could be measured. *B*: plot of normalized eIPSC peak amplitude (mean ± MSE) in the train for 5 experiments similar to those shown in *A*. Note again that the 1st eIPSC increased after CGP55845 but then the response tended to stabilize around the control level (mean ± MSE). The histogram represents charge transfer during the trains, showing no relevant difference between control (white bar) and CGP55845 (black bar) ($P = 0.88$, paired *t*-test). *C*: the paired-pulse ratio (PPR) and CV changes after CGP55845 perfusion are plotted vs. peak amplitude changes (filled circles). In both plots, the data show a linear negative correlation (gray lines; $R^2 = 0.91$, $P < 0.01$, paired *t*-test; $R^2 = 0.89$, $P < 0.01$, paired *t*-test). The points corresponding to the average change in PPR and CV obtained by raising $[Ca^{2+}]_o$ from 0.5 to 2 mM lay in proximity of the CGP data (open circles, mean ± MSE, $n = 5$).

high-affinity GABA$_B$ receptor blocker CGP55845, which is reported to act preferentially on presynaptic GABA$_B$ receptors (Chen and Yung 2005; Fearon et al. 2003; Jensen et al. 1999; Kaneda and Kita 2005; Than and Szabo 2002; Yamada et al. 1999). Another GABA$_B$ receptor antagonist, CGP35348 (Deisz et al. 1997; Morishita and Sastry 1995; Mouginot et al. 1998), was not used since it is known to block postsynaptic GABA$_B$ receptors at the Golgi cell–granule cell synapses and could generate spurious effects on eIPSCs (Rossi et al. 2006). In five experiments, low-concentration (1 μM) CGP55845 modified the eIPSC trains in a characteristic and significant manner (Fig. 6*A*). Whereas the first eIPSC increased by 29.6 ± 9.0% ($n = 5$, $P < 0.03$, paired *t*-test), the second eIPSC in the train did not and PPR decreased by 55.7 ± 12% ($n = 5$, $P < 0.05$, paired *t*-test). Then, nearly the same steady-state amplitude as in control trains was attained within three to four impulses (Fig. 6*B*).

GABA$_B$ receptor blockage increases release probability

The fact that GABA$_B$ receptor blockage increased the first eIPSC and decreased PPR suggested that neurotransmitter release was enhanced. To investigate the mechanism of CGP55845 action, the PPR and CV changes were plotted versus the amplitude change (Fig. 6*C*). In both cases the data showed a significant negative correlation (for PPR, $R^2 = 0.91$, $P < 0.01$, paired *t*-test; for CV, $R^2 = 0.89$ $P < 0.01$, paired *t*-test), consistent with an increase in release probability as the major factor responsible for the CGP55845 effect. Consistently, in the $[M_2/M_1$ vs. $(CV_2/CV_1)^{-2}]$ plot, the experimental points fell above the diagonal, as expected from an increase in quantal release (Fig. 7*A*). The calculation of p using *Eq. 2* yielded an increase from $p = 0.42 \pm 0.08$ to $p = 0.67 \pm 0.09$ ($n = 5$, $P < 0.05$, paired *t*-test) (Fig. 7*B*).

The mechanistic relationship between CGP55845 action and a change in release probability was further supported by the similar location, in all these graphs (Figs. 6*C* and 7, *A* and *B*), of points obtained by increasing release probability with an increase in extracellular calcium. To this aim, a comparison is explicitly shown for transition from 0.5 to 2 mM calcium, since this matches the eIPSC amplitude variation observed after CGP perfusion, although qualitatively similar results were also obtained by using a change from 2 to 4 mM calcium (data not shown). The relationship between CGP55845 and calcium changes was further assessed by using variance/mean analysis. When the variance/mean points for subsequent eIPSC in the trains were reported in Fig. 4*A*, which was constructed at different calcium concentrations, the points obtained both before and after CGP55845 perfusion fell along the same parabolic trajectory (*Eq. 1*). This observation further supported the conclusion that the changes occurring with CGP55845 were caused by an increase in release probability (Fig. 7*C*; cf. e.g., Sola et al. 2004).

Consistent with an increased release probability, mIPSCs recorded in 3 μM TTX (Fig. 7*D*) significantly increased their frequency (39.3 ± 7.9%, $n = 6$; unpaired *t*-test, $P < 0.008$), although their amplitude remained unchanged (0.6 ± 2.8%, $n = 6$; unpaired *t*-test, $P = 0.37$).

Frequency dependence of GABA$_B$ receptor blockage and response buildup during repetitive stimulation

Since the trains used in these experiments were delivered every 10 s, the observed CGP55845 modulation on the first IPSC in the trains occurred at low frequency. However, when IPSC changes were measured in the last IPSC in the trains, almost no modulation was observed. This effect was reminis-

Downloaded from www.physiology.org/journal/jn by ${individualUser.givenNames} ${individualUser.surname} (094.161.143.194) on April 5, 2018.
Copyright © 2009 American Physiological Society. All rights reserved.

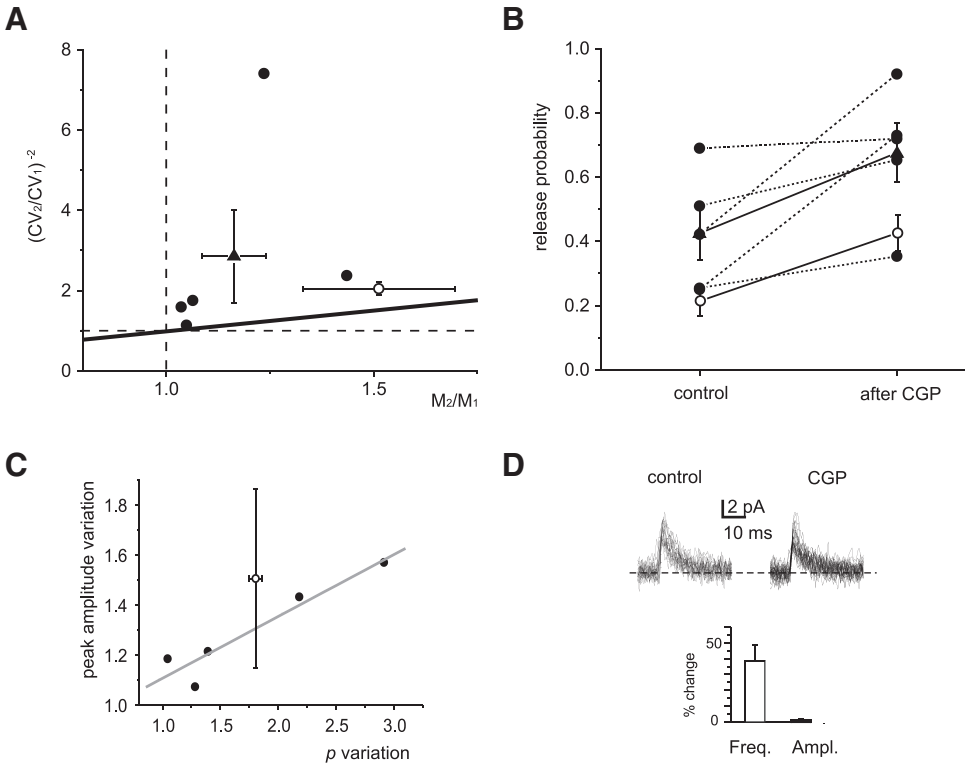

FIG. 7. The effect of $GABA_B$ receptor modulation on release probability. *A*: the plot shows the relationship between $(CV_2/CV_1)^{-2}$ and M_2/M_1 for eIPSCs recorded in control and during CGP55845 perfusion (filled circles indicate single cells; the filled triangle indicates mean ± MSE, $n = 5$). All points fall above the unitary diagonal, i.e., in the sector compatible with a change in release probability. It should be noted that the point corresponding to recordings obtained by raising $[Ca^{2+}]_o$ from 0.5 to 2 mM (open circle, mean ± MSE, $n = 5$) is also in the same sector. *B*: the release probability increase during CGP55845 perfusion is plotted for single cells (filled circles) as well as for their average (filled triangle, mean ± MSE, $n = 5$). The open circles show the average release probability estimated by increasing $[Ca^{2+}]_o$ from 0.5 to 2 mM (mean ± MSE, $n = 5$). *C*: the peak amplitude variation during CGP55845 perfusion is plotted vs. the *p* change. The data show a linear positive correlation (gray line, $R^2 = 0.95$, $P < 0.01$, paired *t*-test). The point obtained by raising $[Ca^{2+}]_o$ from 0.5 to 2 mM (open circle, mean ± MSE, $n = 5$) lays in proximity of the CGP55845 data. The data used for CGP55845 perfusion and calcium concentration changes are the same in all these panels and Fig. 6. *D*: mIPSCs were recorded in the presence of 1 μM TTX either in control or in the presence of CGP55845. mIPSCs did not change their amplitude but increased their frequency ($n = 15$ in control and $n = 22$ in CGP during 7-min recording). The histograms show average changes in mIPSC amplitude and frequency.

cent of that reported at the parent synapse between mossy fibers and granule cells, which is regulated by GABA spillover from the neighboring Golgi cell terminals (Mitchell and Silver 2000b). We therefore reconstructed the frequency dependence of CGP55845 effects by reporting the percentage changes at frequencies between 0.1 and 100 Hz (Fig. 8). It turned out that CGP55845 had a much stronger effect at low frequency than that at high frequency, with a sharp roll-off around 10 Hz. Therefore these results indicate that $GABA_B$ receptor modulation is prevalent during low-frequency transmission.

As noted in Figs. 5*A* and 6*A*, high-frequency 100-Hz IPSC trains showed a pronounced buildup of the response (cf. Rossi et al. 2003). The effectiveness of this temporal summation was monitored through the charge transferred along the trains. No relevant effects of CGP55845 were observed on the total charge transfer ($n = 5$, $P = 0.66$, paired *t*-test; Fig. 6*B*). Likewise, the charge transfer was similar at both 0.5 and 2 mM calcium ($n = 5$, $P = 0.58$, paired *t*-test; Fig. 5*B*). Thus different from IPSC peak amplitude, the transferred charge was almost insensitive to $GABA_B$ receptor blockage and calcium changes. This result indicates that $GABA_B$ receptor regulation of release probability has the initial transient component of the response to a stimulus train as its specific target.

DISCUSSION

In this study we show that, in the juvenile rat cerebellum, GABAergic transmission at the Golgi cell–granule cell synapse is multiquantal. During repetitive stimulation, GABAergic transmission undergoes short-term depression of a fast transient component, whereas a slow protracted component shows a remarkable buildup due to temporal summation (Rossi and Haman 1998; Rossi et al. 2002). These observations conform to a mechanism of synaptic integration, in which α_1 receptors determine a transient (direct) response to released GABA, whereas α_6 receptors determine slow (indirect) spillover-mediated currents (Cherubini and Conti 2001; Farrant and Nusser 2005; Glykys and Mody 2007). The main finding is that release probability was tonically reduced by $GABA_B$ receptor activation. This regulation was typically expressed at low frequency (0.1–10 Hz) but became undetectable at high frequency (100 Hz). During high-frequency trains, $GABA_B$ receptor-mediated regulation was evident in the first IPSC but no longer so after a few impulses, either in the transient component or in the slow component. Thus ambient GABA in the glomerulus could act presynaptically on Golgi cell $GABA_B$ autoreceptors selectively regulating the onset of inhibition.

Downloaded from www.physiology.org/journal/jn by ${individualUser.givenNames} ${individualUser.surname} (094.161.143.194) on April 5, 2018.
Copyright © 2009 American Physiological Society. All rights reserved.

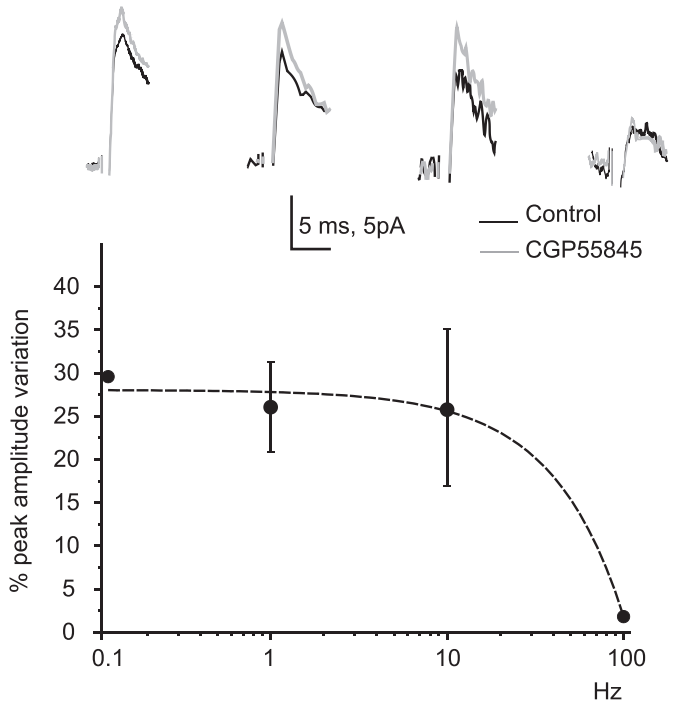

FIG. 8. Frequency dependence of GABA$_B$ receptor blockage. The *top traces* show eIPSCs elicited at different frequencies in control and during CGP55845 perfusion. Note the eIPSC increase at 0.1, 1, and 10 Hz but not at 100 Hz. The plot shows average changes in eIPSC amplitude at different stimulation frequencies.

Quantal properties of neurotransmission at the Golgi cell–granule cell synapse

The Golgi cell–granule cell synapse conformed to a general model of multiquantal neurotransmission, in which IPSC amplitude fluctuations are mostly generated by the variable number of quantal events occurring at multiple releasing sites (Cherubini and Conti 2001; Edwards et al. 1990). Although at other inhibitory synapses minis could be multiquantal (Auger and Marty 2000; Auger et al. 1998; Glykys and Mody 2007), this is probably not the case at the Golgi cell–granule cell synapse, since minis have fast nonindented rising phases and coincide with the uniquantal eIPSCs measured in low-calcium solutions. Moreover, with a quantum conductance of 214 pS, a single-channel conductance of 30 pS and an open probability of 0.6 (for a critical review on these parameters see Farrant and Nusser 2005), it can be estimated that around 10 GABA$_A$ α_1 subunit-containing channels are present in the postsynaptic density and about 80% of them are open at peak. With these parameters, a quantum is associated with an intrasite variance ($cv_{I\text{-}ss}$) of 0.16, in line with the expectation that $cv_{I\text{-}ss}$ is about half of the quantum variance cv_q (Clements 2003). Thus statistical fluctuations of minis amplitude are consistent with the hypothesis that, at the Golgi cell–granule cell synapse, release occurs in single rather than aggregated quanta, suggesting a nearly saturated model of postsynaptic receptor activation.

Assuming independent release of multiple quanta, MPFA yielded an average release probability $p = 0.32$ and an average number of releasing sites $n = 4.7$ (standard extracellular calcium concentration, 2 mM). The quantum size obtained with MPFA was in fair agreement with the average minis size and p almost coincided with the values yielded by failure rate and CV calculations (see Fig. 4*B*), providing a cross-validation of the different methods and supporting the conformity of the system to simple binomial statistics (e.g., see MacLachian 1978; Saviane and Silver 2006a,b). The consistency of quantal parameter estimates was presumably enhanced by the availability of single quantum properties extracted from independent minis measurements, by the secure identification of minimal eIPSCs through a comparison with sIPSCs and by the selection of transmission failures through the indirect eIPSC component. The multiquantal nature of neurotransmission is supported by the expectation-maximization (EM) observation that Golgi cell axon terminals make multiple contacts containing several synaptic vesicles on different dendritic digits on the same granule cell dendrite (Hámori and Somogy 1983; Hámori and Szentagothai 1966; Jakab and Hámori 1988). Additional EM analysis may be useful to estimate the number of morphologically identified active zones and postsynaptic receptor density. Moreover, the contribution of GABA$_A$ receptor desensitization to the IPSC trains may be estimated using computational modeling of neurotransmission (Nieus and D'Angelo, unpublished observations).

The small size of the inhibitory synaptic currents should not be surprising. The single quantum conductance (214 pS) is relatively large compared with the resting whole cell conductance (~1,000 pS; Arenz et al. 2008; Armano et al. 2000; D'Angelo et al. 1995; Rancz et al. 2007), so that even a single quantum can determine a remarkable inhibitory effect contrasting the depolarization caused by excitatory synapses. The proposed synaptic arrangement and release statistics are similar to those of the neighboring mossy fiber–granule cell synapse (Saviane and Silver 2006a,b; Sola et al. 2004), indicating that the glomerular system can provide an appropriate excitatory/inhibitory balance to the granule cells.

Regulation of release probability by tonic GABA$_B$ receptor activation

GABA$_B$ receptors blockage increased release probability and, accordingly, increased the first eIPSC and accentuated short-term depression in eIPSC trains. Moreover, minis frequency (but not minis amplitude) also increased. A prediction from such presynaptic mechanism is that p variations and associated IPSC amplitude changes should be larger with low initial release probability. Another prediction is that PPR and CV changes should be negatively correlated with IPSC amplitude variation. Actually, all these correlations proved statistically significant and points in the $[M_2/M_1$ vs. $(CV_1/CV_2)^{-2}]$ plot fell above the unitary diagonal, as expected from an increase in quantal release. The range of responses to GABA$_B$ receptor blockage may reflect regulation of ambient GABA levels (Farrant and Nusser 2005; Hamann et al. 2002) or variable efficiency of the transduction cascades involving GABA$_B$ receptors.

The effects of the GABA$_B$ receptor antagonist CGP55845 were similar to those caused by increasing extracellular Ca^{2+}, consistent with the observation that CGP55845 preferentially inhibits presynaptic GABA$_B$ receptors (Yamada et al. 1999; see also Chen and Yung 2005; Fearon et al. 2003; Jensen et al. 1999; Kaneda and Kita 2005; Than and Szabo 2002). Moreover, the action of CGP55845, by occurring in the first response in a train, reveals the blockage of GABA$_B$ receptors that were tonically activated. The estimated ambient GABA level in the cerebellar glomerulus is 10^{-8}–10^{-6} M (Farrant and Nusser 2005) and can therefore activate presynaptic GABA$_B$ receptors, which have EC_{50} in the

Downloaded from www.physiology.org/journal/jn by ${individualUser.givenNames} ${individualUser.surname} (094.161.143.194) on April 5, 2018.
Copyright © 2009 American Physiological Society. All rights reserved.

same concentration range (Galvez et al. 2000). Given the strong analogy with the presynaptic effects of Ca^{2+}, it is possible that the *p* reduction caused by $GABA_B$ receptors involves G-protein–dependent inhibition of voltage-dependent calcium currents, as reported at other central synapses (Dittman and Regehr 1996; Takahashi et al. 1998). A slowing down of vesicle recycling (Sakaba and Neher 2003) might occur along the short trains used for synaptic stimulation in our recordings, thus explaining the absence of CGP modulation at high-frequency. Finally, it should be noted that the mechanism of presynaptic GABAergic regulation may not be the same at other brain synapses. For instance, at inhibitory synapses of the hippocampus, GABA receptors have been reported to exert their presynaptic effect independent from a change in release probability (Hefft et al. 2002).

In aggregate, these results indicate that $GABA_B$ receptors in Golgi cells (Kulik et al. 2002) are expressed in presynaptic terminals, where they are tonically activated by ambient GABA and negatively regulate neurotransmitter release. Although a tonic presynaptic inhibition of neurotransmitter release by $GABA_B$ receptor was also reported at other central synapses (Chen and Yung 2005; Fearon 2003; Jensen et al. 1999; Morishita and Sastry 1995; Mouginot et al. 1998; Porter and Nieves 2004), in the cerebellar glomerulus this mechanism would benefit from restricted neurotransmitter diffusion, which can also favor cross talk between glutamatergic and GABAergic terminals. In particular, metabotropic glutamate receptors can inhibit GABA release from Golgi cell terminals and $GABA_B$ receptors can inhibit glutamate release from mossy fiber (Mitchell and Silver 2000a,b). Moreover, $GABA_B$ receptors are also expressed postsynaptically, where they can regulate granule cell input resistance through a modulation of inward rectifier channels (Rossi et al. 2006). The frequency dependence of these processes is also peculiar, in that presynaptic $GABA_B$ receptor-mediated regulation at both excitatory and inhibitory terminals occurs at low frequency (when only tonic GABA levels are relevant), whereas that of granule cell conductance occurs at high frequency (therefore requiring GABA buildup during repetitive neurotransmission). Finally, it should be noted that ambient GABA levels have been reported to regulate granule cell input resistance (Brickley et al. 1996) and mossy fiber–granule cell gain (Mitchell and Silver 2003) through tonic activation of $GABA_A$ receptors. Thus presynaptic control by $GABA_B$ autoreceptors on Golgi cell terminals appears as a part of a more complex system based on ambient GABA levels and spillover suited to control multiple aspects of glomerular signal processing.

Functional implications and potential impact on granular layer functions

The rapid activation of IPSC is well suited to explain Golgi cell–granule cell inhibition reported in vivo in the adult cat (see Eccles et al. 1967). Presynaptic $GABA_B$ receptor-mediated control of release probability can be regarded as a mechanism to regulate the sharpness of the onset of inhibition. This effect is better conceived within the time-window hypothesis (D'Angelo and DeZeeuw 2008; Kistler and DeZeeuw 2003; Mapelli and D'Angelo 2007), which assumes that Golgi cell feedforward inhibition can limit the discharge of connected granule cells within about 5 ms. Low ambient GABA and $GABA_B$ receptor activation would sharply delimit the time window, during which granule cell spikes have the highest probability of being generated. Moreover, since the ambient GABA level is proportional to Golgi cells' background activity (Rossi et al. 2003), these same granule cells will also have lower $GABA_A$ receptor-mediated noise and leakage (Brickley et al. 1996), resulting in higher precision and intensity of their response to mossy fiber activation. This temporally limited and precise discharge would then improve the pattern recognition process that is thought to take place in Purkinje cells (Brunel et al. 2004; Steuber et al. 2007). The impact of these time-filtering mechanisms needs to be further investigated using large-scale detailed network models and multisite and imaging recordings of network activity.

ACKNOWLEDGMENTS

We thank Dr. S. Solinas for the contribution to statistical analysis and A. Lüthi for comments on the manuscript.

GRANTS

This work was supported by the European Union Grant SENSOPAC FP6-IST028056 and by National Consortium for the Physics of Matter Grant NEUROIMAGE.

REFERENCES

Arenz A, Silver RA, Schaefer AT, Margrie TW. The contribution of single synapses to sensory representation in vivo. *Science* 321: 977–980, 2008.

Armano S, Rossi P, Taglietti V, D'Angelo E. Long-term potentiation of intrinsic excitability at the mossy fibre–granule cell synapse of rat cerebellum. *J Neurosci* 20: 5208–5216, 2000.

Auger C, Kondo S, Marty A. Multivesicular release at single functional synaptic sites in cerebellar stellate and basket cells. *J Neurosci* 18: 4532–4547, 1998.

Auger C, Marty A. Quantal currents at single-site central synapses. *J Physiol* 526: 3–11, 2000.

Brickley SG, Cull-Candy SG, Farrant M. Development of a tonic form of synaptic inhibition in rat cerebellar granule cells resulting from persistent activation of $GABA_A$ receptors. *J Physiol* 497: 753–759, 1996.

Brickley SG, Cull-Candy SG, Farrant M. Single-channel properties of synaptic and extrasynaptic $GABA_A$ receptors suggest differential targeting of receptor subtypes. *J Neurosci* 19: 2960–2973, 1999.

Brunel N, Hakim V, Isope P, Nadal JP, Barbour B. Optimal information storage and the distribution of synaptic weights: perceptron versus Purkinje cell. *Neuron* 43: 745–757, 2004.

Chatala L, Brickley S, Cull-Candy S, Farrant M. Maturation of EPSCs and intrinsic membrane properties enhances precision at a cerebellar synapse. *J Neurosci* 23: 6074–6085, 2003.

Chen L, Yung W. Tonic activation of presynaptic GABA(B) receptors on rat pallidosubthalamic terminals. *Acta Pharmacol Sin* 26: 10–16, 2005.

Cherubini E, Conti F. Generating diversity at GABAergic synapses. *Trends Neurosci* 24: 155–162, 2001.

Clements JD. Variance-mean analysis: a simple and reliable approach for investigating synaptic transmission and modulation. *J Neurosci Methods* 130: 115–125, 2003.

Clements JD, Silver RA. Unveiling synaptic plasticity: a new graphical and analytical approach. *Trends Neurosci* 23: 105–113, 2000.

D'Angelo E, De Filippi G, Rossi P, Taglietti V. Synaptic excitation of individual rat cerebellar granule cells in situ: evidence for the role of NMDA receptors. *J Physiol* 484: 397–413, 1995.

D'Angelo E, De Zeeuw CI. Timing and plasticity in the cerebellum: focus on the granular layer. *Trends Neurosci* 32: 30–40, 2008.

D'Angelo E, Nieus T, Maffei A, Armano S, Rossi P, Taglietti V, Fontana A, Naldi G. Theta-frequency bursting and resonance in cerebellar granule cells: experimental evidence and modeling of a slow K^+-dependent mechanism. *J Neurosci* 21: 759–770, 2001.

D'Angelo E, Rossi P, Armano S, Taglietti V. Evidence for NMDA and mGlu receptor-dependent long-term potentiation of mossy-fiber-granule cell transmission in rat cerebellum. *J Neurophysiol* 81: 277–287, 1999.

D'Angelo E, Rossi P, Taglietti V. Different proportions of N-methyl-D-aspartate receptor currents at the mossy fibre–granule cell synapse of developing rat cerebellum. *Neuroscience* 53: 121–130, 1993.

Deisz RA, Billard JM, Zieglgänsberger W. Presynaptic and postsynaptic $GABA_B$ receptors of neocortical neurons of the rat in vitro: differences in pharmacology and ionic mechanisms. *Synapse* 25: 62–72, 1997.

Downloaded from www.physiology.org/journal/jn by ${individualUser.givenNames} ${individualUser.surname} (094.161.143.194) on April 5, 2018.
Copyright © 2009 American Physiological Society. All rights reserved.

DiGregorio DA, Nusser Z, Silver RA. Spillover of glutamate onto synaptic AMPA receptors enhances fast transmission at a cerebellar synapse. *Neuron* 35: 521–533, 2002.

Dittman JS, Regehr WG. Contributions of calcium-dependent and calcium-independent mechanisms to presynaptic inhibition at a cerebellar synapse. *J Neurosci* 16: 1623–1633, 1996.

Dodge FA Jr, Rahamimoff R. Co-operative action a calcium ions in transmitter release at the neuromuscular junction. *J Physiol* 193: 419–432, 1967.

Dutar P, Nicoll R. A physiological role for $GABA_B$ receptors in the central nervous system. *Nature* 332: 156–158, 1988.

Eccles JC, Ito M, Szentagothai J. *The Cerebellum as a Neuronal Machine*. Berlin: Springer-Verlag, 1967.

Edwards FA, Konnerth A, Sakmann B. Quantal analysis of inhibitory synaptic transmission in the dentate gyrus of rat hippocampal slices: a patch-clamp study. *J Physiol* 430: 213–249, 1990.

Farrant M, Nusser Z. Variations on an inhibitory theme: phasic and tonic activation of $GABA_A$ receptors. *Nat Rev Neurosi* 6: 215–229, 2005.

Fearon IM, Zhang M, Vollmer C, Nurse CA. GABA mediates autoreceptor feedback inhibition in the rat carotid body via presynaptic $GABA_B$ receptors and TASK-1. *J Physiol* 553: 83–94, 2003.

Forti L, Cesana E, Mapelli J, D'Angelo E. Ionic mechanisms of autorhythmic firing in rat cerebellar Golgi cells. *J Physiol* 574: 711–729, 2006.

Galvez T, Urwyler S, Prézeau L, Mosbacher J, Joly C, Malitschek B, Heid J, Brabet I, Froestl W, Bettler B, Kaupmann K, Pin JP. Ca^{2+} requirement for high-affinity γ-aminobutyric acid (GABA) binding at GABA-B receptors: involvement of serine 269 of the $GABA_BR1$ subunit. *Mol Pharmacol* 57: 419–426, 2000.

Glykys J, Mody I. Activation of $GABA_A$ receptors: views from outside the synaptic cleft. *Neuron* 56: 763–770, 2007.

Hamann M, Rossi DJ, Attwell D. Tonic and spillover inhibition of granule cells control information flow through cerebellar cortex. *Neuron* 33: 625–633, 2002.

Hámori J, Somogyi J. Differentiation of cerebellar mossy fiber synapses in the rat: a quantitative electron microscope study. *J Comp Neurol* 220: 365–377, 1983.

Hámori J, Szentagothai J. Participation of Golgi neuron processes in the cerebellar glomeruli: an electron microscope study. *Exp Brain Res* 2: 35–48, 1966.

Harvey RJ, Napper RM. Quantitative studies on the mammalian cerebellum. *Prog Neurobiol* 36: 437–463, 1991.

Hefft S, Kraushaar U, Geiger JR, Jonas P. Presynaptic short-term depression is maintained during regulation of transmitter release at a GABAergic synapse in rat hippocampus. *J Physiol* 539: 201–208, 2002.

Jakab RL, Hámori J. Quantitative morphology and synaptology of cerebellar glomeruli in the rat. *Anat Embryol* 179: 81–88, 1988.

Jensen K, Lambert JD, Jensen MS. Activity-dependent depression of GABAergic IPSCs in cultured hippocampal neurons. *J Neurophysiol* 82: 42–49, 1999.

Kaneda K, Kita H. Synaptically released GABA activates both pre- and postsynaptic $GABA_B$ receptors in the rat globus pallidus. *J Neurophysiol* 94: 1104–1114, 2005.

Katz B, Miledi R. Ionic requirements of synaptic transmitter release (Letter). *Nature* 215: 651, 1967.

Kistler WM, DeZeeuw CI. Time windows and reverberating loops: a reverse-engineering approach to cerebellar function. *Cerebellum* 2: 44–54, 2003.

Kulik A, Nakadate K, Nyíri G, Notomi T, Malitschek B, Bettler B, Shigemoto R. Distinct localization of $GABA_B$ receptors relative to synaptic sites in the rat cerebellum and ventrobasal thalamus. *Eur J Neurosci* 15: 291–307, 2002.

Larkman A, Hannay T, Stratford K, Jack J. Presynaptic release probability influences the locus of long-term potentiation. *Nature* 360: 70–73, 1992.

Maffei A, Prestori F, Rossi P, Taglietti V, D'Angelo E. Presynaptic current changes at the mossy fiber–granule cell synapse of cerebellum during LTP. *J Neurophysiol* 88: 627–638, 2002.

Mapelli J, D'Angelo E. The spatial organization of long-term synaptic plasticity at the input stage of cerebellum. *J Neurosci* 27: 1285–1296, 2007.

McLachian EM. The statistics of transmitter release at chemical synapses. *Int Rev Physiol Neurophysiol* 17: 49–117, 1978.

Misgeld U, Bijak M, Jarolimek W. A physiological role for $GABA_B$ receptors and the effects of baclofen in the mammalian central nervous system. *Prog Neurobiol* 46: 423–462, 1995.

Mitchell SJ, Silver RA. Glutamate spillover suppresses inhibition by activating presynaptic mGluRs. *Nature* 404: 498–502, 2000a.

Mitchell SJ, Silver RA. GABA spillover from single inhibitory axons suppresses low-frequency excitatory transmission at the cerebellar glomerulus. *J Neurosci* 20: 8651–8658, 2000b.

Mitchell SJ, Silver RA. Shunting inhibition modulates neuronal gain during synaptic excitation. *Neuron* 38: 433–445, 2003.

Morishita W, Sastry BR. Pharmacological characterization of pre- and postsynaptic $GABA_B$ receptors in the deep nuclei of rat cerebellar slices. *Neuroscience* 68: 1127–1137, 1995.

Mouginot D, Kombian SB, Pittman QJ. Activation of presynaptic $GABA_B$ receptors inhibits evoked IPSCs in rat magnocellular neurons in vitro. *J Neurophysiol* 79: 1508–1517, 1998.

Nicoll RA. My close encounter with $GABA_B$ receptors. *Biochem Pharmacol* 68: 1667–1674, 2004.

Nieus T, Sola E, Mapelli J, Saftenku E, Rossi P, D'Angelo E. Regulation of repetitive neurotransmission and firing by release probability at the input stage of cerebellum: experimental observations and theoretical predictions on the role of LTP. *J Neurophysiol* 95: 686–699, 2006.

Porter JT, Nieves D. Presynaptic $GABA_B$ receptors modulate thalamic excitation of inhibitory and excitatory neurons in the mouse barrel cortex. *J Neurophysiol* 92: 2762–2770, 2004.

Rancz EA, Ishikawa T, Duguid I, Chadderton P, Mahon S, Häusser M. High-fidelity transmission of sensory information by single cerebellar mossy fibre boutons. *Nature* 450: 1245–1249, 2007.

Rossi DJ, Hamann M. Spillover-mediated transmission at inhibitory synapses promoted by high affinity alpha6 subunit $GABA_A$ receptors and glomerular geometry. *Neuron* 20: 783–795, 1998.

Rossi DJ, Hamann M, Attwell D. Multiple modes of GABAergic inhibition of rat cerebellar granule cells. *J Physiol* 548: 97–110, 2003.

Rossi P, Mapelli L, Roggeri L, Gall D, de Kerchove d'Exaerde A, Schiffmann SN, Taglietti V, D'Angelo E. Inhibition of constitutive inward rectifier currents in cerebellar granule cells by pharmacological and synaptic activation of GABA receptors. *Eur J Neurosci* 24: 419–432, 2006.

Sakaba T, Neher E. Direct modulation of synaptic vesicle priming by $GABA_B$ receptor activation at a glutamatergic synapse. *Nature* 424: 775–778, 2003.

Saviane C, Silver RA. Fast vesicle reloading and a large pool sustain high bandwidth transmission at a central synapse. *Nature* 439: 983–987, 2006a.

Saviane C, Silver RA. Errors in the estimation of the variance: implications for multiple-probability fluctuation analysis. *J Neurosci Methods* 153: 250–260, 2006b.

Silver RA. Estimation of nonuniform quantal parameters with multiple-probability fluctuation analysis: theory, application and limitations. *J Neurosci Methods* 130: 127–141, 2003.

Silver RA, Cull-Candy SG, Takahashi T. Non-NMDA glutamate receptor occupancy and open probability at a rat cerebellar synapse with single and multiple release sites. *J Physiol* 494: 231–250, 1996.

Sola E, Prestori F, Rossi P, Taglietti V, D'Angelo E. Increased neurotransmitter release during long-term potentiation at mossy fibre-granule cell synapses in rat cerebellum. *J Physiol* 557: 843–861, 2004.

Solinas S, Forti L, Cesana E, Mapelli J, De Schutter E, D'Angelo E. Fast-reset of pacemaking and theta-frequency resonance patterns in cerebellar Golgi cells: simulations of their impact *in vivo*. *Front Cell Neurosci* 1: Article 4, 2007a.

Solinas S, Forti L, Cesana E, Mapelli J, De Schutter E, D'Angelo E. Computational reconstruction of pacemaking and intrinsic electroresponsiveness in cerebellar Golgi cells. *Front Cell Neurosci* 1: Article 2, 2007b.

Steuber V, Mittmann W, Hoebeek FE, Silver RA, De Zeeuw CI, Häusser M, De Schutter E. Cerebellar LTD and pattern recognition by Purkinje cells. *Neuron* 54: 121–136, 2007.

Takahashi T, Kajikawa Y, Tsujimoto T. G-protein-coupled modulation of presynaptic calcium currents and transmitter release by a $GABA_B$ receptor. *J Neurosci* 18: 3138–3146, 1998.

Than M, Szabo B. Analysis of the function of $GABA_B$ receptors on inhibitory afferent neurons of Purkinje cells in the cerebellar cortex of the rat. *Eur J Neurosci* 15: 1575–1584, 2002.

Tia S, Wang JF, Kotchabhakdi N, Vicini S. Developmental changes of inhibitory synaptic currents in cerebellar granule neurons: role of GABA(A) receptor alpha 6 subunit. *J Neurosci* 16: 3630–3640, 1996.

Vos BP, Volny-Luraghi A, De Schutter E. Cerebellar Golgi cells in the rat: receptive fields and timing of responses to facial stimulation. *Eur J Neurosci* 11: 2621–2634, 1999.

Wall MJ. Furosemide reveals heterogeneous $GABA_A$ receptor expression at adult rat Golgi cell to granule cell synapses. *Neuropharmacology* 43: 737–749, 2002.

Yamada K, Yu B, Gallagher JP. Different subtypes of $GABA_B$ receptors are present at pre- and postsynaptic sites within the rat dorsolateral septal nucleus. *J Neurophysiol* 81: 2875–2883, 1999.

Downloaded from www.physiology.org/journal/jn by ${individualUser.givenNames} ${individualUser.surname} (094.161.143.194) on April 5, 2018.
Copyright © 2009 American Physiological Society. All rights reserved.